Ultrasound pulse measurement of air-lift multiphase pipe flow in an inclined pipe

Yuichi Murai[1], Takumi Hayashi[1], Dongik Yoon[1], Hyun Jin Park[1], Yuji Tasaka[1], Satoru Takano[2], and Sotaro Masanobu[3]

[1] Faculty of Engineering, Hokkaido University, N13W8, Sapporo 060-8628, Japan
[2] Ocean Engineering Department, National Maritime Research Institute, Mitaka, Tokyo 181-0004, Japan
[3] Offshore Advanced Technology Department, National Maritime Research Institute, Mitaka, Tokyo 181-0004, Japan

We developed the method of ultrasonic detection for large bubbles rising rapidly in an upward gas–liquid two-phase pipe flow at a variable inclination angle. The proposed method uses combination of the echo intensity reflected by large bubbles and the Doppler frequency. The method using the Doppler frequency performs well in the detection of large bubbles regardless of the interface condition, whereas the method using the echo intensity has trouble in detecting an uneven interface. In contrast, the information of the echo intensity guarantees high accuracy of the interface detection even if that of the Doppler frequency has low accuracy for the detection owing to many small bubbles existing in the liquid film. Here, the two methods are combined to overcome their problems, and a validation test confirms that the results of the combined method agree well with the results of image processing. As demonstrations of the proposed method, the slug frequency, velocity, and airflow rate of large bubbles in an air-lift pump are obtained.

Keywords: Air-lift pump, three-phase flow, bubble velocity, liquid film, flow-metering, pressure loss

1. Introduction

Multiphase flow plays an important role in many practical fields such as oil transportation, chemical engineering, and airlift pumps. Slug flow is a common flow pattern that appears widely in two-phase flow where bubbles become large enough to occupy almost the entire pipe cross-section. The characteristics of slug flow with a high superficial velocity of the gas phase (j_g) are completely different from those of the Taylor bubble that rises smoothly keeping axisymmetric interfacial figures. In air-lift pumps, typical speed of the bubbles exceeds 3 m/s and the gas-liquid interface experiences highly unsteady three-dimensional turbulence[1-4]. In this study, we have developed a method to capture such an interface using combined capabilities of ultrasound echo intensity and Doppler signal information based on the knowledge of ultrasonic interfacial detection[5-10].

2. Experimental Method

2.1 Experimental facility

The airlift pump system at the National Maritime Research Institute (NMRI, Japan) is used in the present study (Fig. 1). The total height (H) of the main pipe was 8.5 m and the inner diameter (D) was 26 mm. The inclination of the pipe (θ) could be freely controlled from 45◦ to 90◦. Compressed air was injected into the bottom of the pipe at a fixed flow rate controlled by an electronic valve, and a flowmeter monitored the flow rate. The main pipe was filled with water and the water level was maintained by a water level adjuster next to the main pipe. The injected air was discharged at the outlet of the pipe, and the lifted water was discharged to a top water tank along a guide vane. The liquid flow rate was estimated by measuring the mass of stored water in the tank, and the superficial velocity of liquid flow (j_l) was obtained from the flow rate. The top tank allowed only water to enter the bottom water tank.

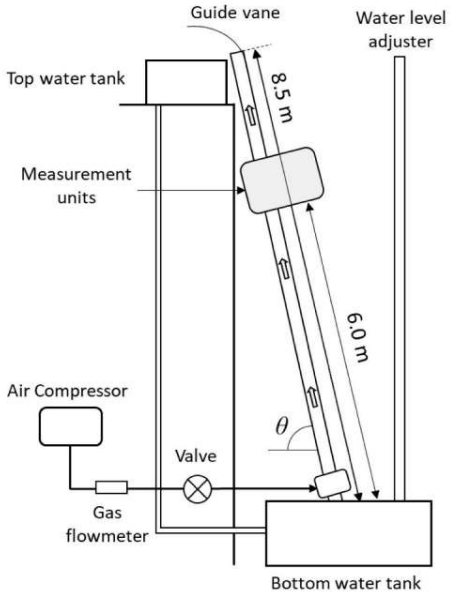

Figure 1: The experimental set-up of an air-lift pump system allowing variable inclination angle at $45<\theta<90$ degree.

2.2 Ultrasound Sensing

The measurement units comprised two US measurement sets with one optical measurement system as shown in Fig. 2. Two US transducers (TDX1 and TDX2) were installed in each water jacket made from transparent acrylic resin, and they were sufficiently submerged in water to avoid exposure to air. Both transducers were placed 30 mm from

the outer wall of the pipe to avoid the near-field effect. The scattering reflection of large bubbles occurs at nose regions because of its curved interface, and it results in echo signal loss. Therefore, we determine the optimal angle of both TDXs as 3◦ based on our previous study that measured the large bubbles using ultrasound measurement [4, 6]. The distance (lTDX) between the centers of TDX1 and TDX2 was 500 mm. Large bubbles with high j_g are asymmetric in the inclined pipe, and the thickness of the liquid film was thus different on the two sides. Accordingly, TDX1 and TDX2 were installed on opposite sides of the pipe to measure the thickness on both sides. A high-speed camera and light-emitting diode panel were installed at the same position as TDX2 for comparison with the US measurement.

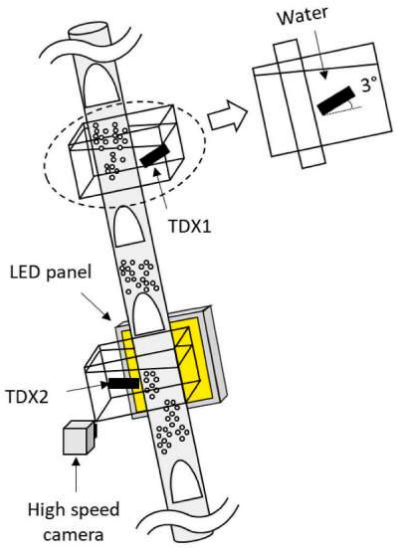

Figure 2: Location of ultrasound transducer to measure the asymmetric multiphase flow inside the inclined pipe.

2.3 Experimental conditions

The experiments were conducted using three superficial velocities of the gas-phase flow (j_g = 1.67, 3.71, 4.95 m/s). Since the US measurements utilized in many industries involving inclined conditions, three inclinations (θ = 45◦, 75◦, 90◦) were thus adopted. j_l is varied by not only θ but also j_g, and the range of j_l was 0.70–1.05 m/s. Note that the flow pattern falls in the slug flow regime and does not change remarkably as shown in Fig. 3. All other details of the experimental conditions are listed in Table 1.

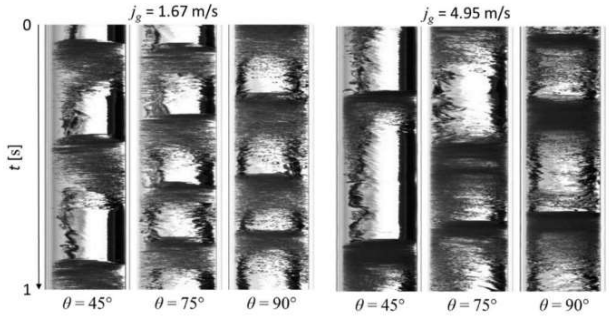

Figure 3: Timeline images of the gas−liquid two-phase flow produced by image processing of high-speed video camera.

Table 1: Experimental and measurement conditions

Flow conditions		
Inner diameter of pipe (D)	26	mm
Pipe length (L)	8.5	m
Inclination of pipe (θ)	45, 75, 90	degrees
Superficial velocity of gas-phase (j_g)	1.67, 3.71, 4.95	m/s
Superficial velocity of liquid-phase (j_l)	0.70–1.05	m/s
Water temperature	21	°C
Measurement conditions		
Measurement position (l/D)	250	
Ultrasound frequency (f_0)	4.187	MHz
Pulse repetition frequency (f_{PRF})	3.998	kHz
Cycles of ultrasound pulse	4	
Emission voltage of ultrasound	60	V
Gain value of US generators	+20	dB
Recording range of voltage (V_{range})	500	mV
Speed of sound (c)	1480	m/s
Sampling speed of US signal (t_s)	40	ns
Spatial resolution of US signal ($\Delta\xi$)	29.4	μm
Measurement time	10	s
Angles of TDX	3	degrees
Frame rate of the camera	500	Fps

3. Experimental Results

3.1 Time-line visualization

From each ultrasound transducer, we could obtain echo intensity and Doppler velocity as a function of time. These original data are shown in Fig. 4 for the vertical pipe and Fig. 5 for 45-deg inclined pipe. The velocity profile is estimated using two successive pulses (e.g., the first and second pulses, the second and third pulses, and the third and fourth pulses), and the temporal resolution of the velocity profile is thus the same as that of the raw echo signals (TDX2-Echo). The liquid velocity remarkably fluctuates with the measurement time for dispersed bubbles passing the US beam whereas more than half of values of the liquid velocity are almost zero for the large bubbles on the US beam. The variance of velocity (TDX2-Var) is estimated for further analysis of the fluctuation of the liquid velocity. A blue line in TDX2-Var represents the variance whereas a red line represents the moving average of the variance using 80 windows, with the corresponding t being 0.02 s.

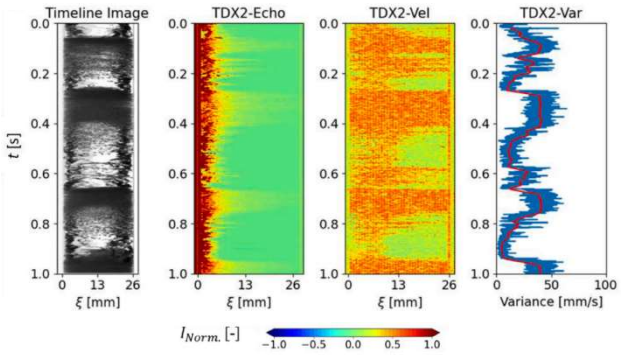

Figure 4: Timeline ultrasonic echogram and Doppler map at j_g =3.71 m/s and θ = 90◦.

Under the vertical condition (Fig. 4), it is clearly seen that the variance is high at the dispersed bubbles whereas it is low at the large bubbles as determined by comparing with the timeline image. However, this trend becomes unclear at θ = 45◦ (Fig. 5). This is due to the small bubbles in the liquid film. The thickness of the liquid film increases with a reduction of inclination, and the bubbles are entrained in the film. The bubbles dispersed in

the liquid film lead to a high variation in the Doppler frequency, and the variance does not vary remarkably compared with the variance at θ = 90◦. To conclude, the variance depends on the number of bubbles dispersed in the liquid film, and the number density of bubbles in the film increases with the reduction of θ resulting in errors in the detection of large bubbles.

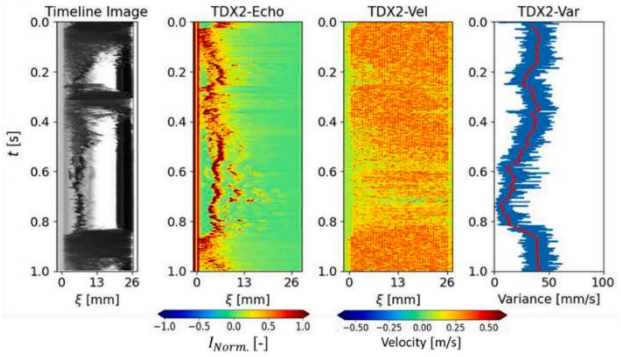

Figure 5: Timeline ultrasonic echogram and Doppler map at j_g =3.71 m/s and θ = 45◦.

3.2 Combined algorithm

The results for the detection of large bubbles using the information of echo intensity and Doppler frequency are shown in Fig. 6. The grey and green regions indicate the detection of a large bubble by the methods using information on the echo intensity and Doppler frequency. Although both methods identify the large bubble, they fail sometimes to recognize the bubble. We consider two combination algorithms, namely the AND OR algorithms. In the AND algorithm, a large bubble is detected if both methods share part of the detection of the large bubble, and the passing times of the large bubble in the nose and tail are determined by the entrained small bubbles in the liquid film (see the red line). Meanwhile, the method using the echo intensity identifies the large bubble despite the existence of small bubbles in the film. The echo intensity reflected by small bubbles is removed by the median filter, leaving only echo signals reflected by the large bubble. In summary, both methods are likely to involve large errors when they are solely used owing to the above described issues. However, their combination cancels out each other's drawbacks. We have overcome the issue with comparison by optical measurement and applied the most suitable thresholds for each ultrasound signals. Details are reported in our previous paper [4, 11, 12].

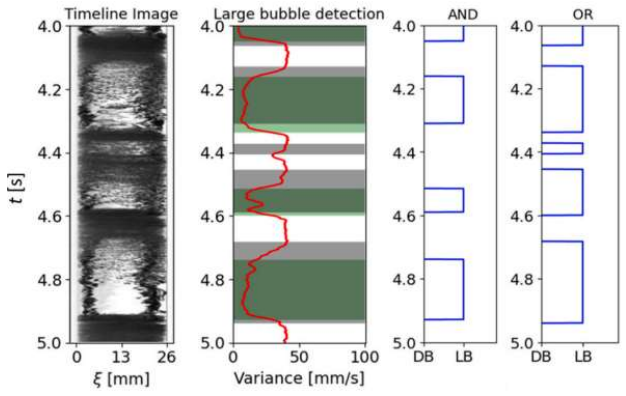

Figure 6: Comparison of AND OR algorithms for large bubble detection at j_g= 3.71 m/s and θ = 90◦.

3.3 Statistics and discussion

Fig. 7 shows the probability of the slug frequency obtained from (a) the proposed method and (b) brightness information of optical measurement with the colors of the graphs indicating j_g. For the result of US measurement, a common feature among the graphs is that f_s is densely distributed at low frequencies with j_g= 1.67 m/s whereas the distribution tends to become wide with an increase in j_g at all inclinations. This trend agrees with the result of Murai et al. that the mean f_s increases with j_g [4]. Meanwhile, f_s at θ = 75◦–90◦ has a similar distribution between j_g = 1.67 m/s and j_g = 3.71 m/s, whereas f_s at θ = 45◦ has a similar distribution between j_g =3.71 m/s and j_g = 4.95 m/s. This indicates that the length and velocity of the large bubble appreciably vary at 45◦ = θ ≤ 75◦. In other words, f_s depends on both the inclination of the pipe and the superficial velocity of the gas flow. In the comparison of the US and optical measurements, f_s at j_g = 1.67 m/s and 3.71 m/s obtained from both measurements in all θ shows similar trends to each other, although the probability is slightly different. Meanwhile, f_s at j_g = 4.95 m/s obtained from optical measurement is more densely distributed than that of US measurement. It is supposed that the minor differences between both measurements come from the definition of the large bubble.

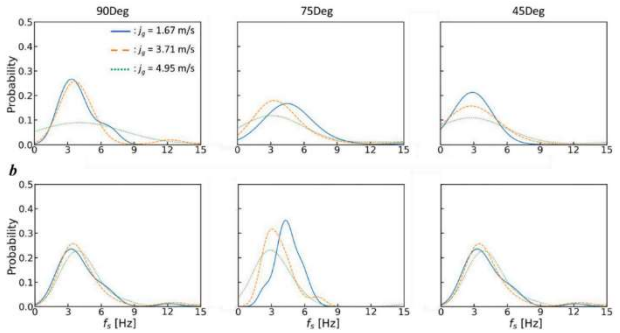

Figure 7. Probability of the slug frequency obtained from (a) proposed method and (b) optical measurement.

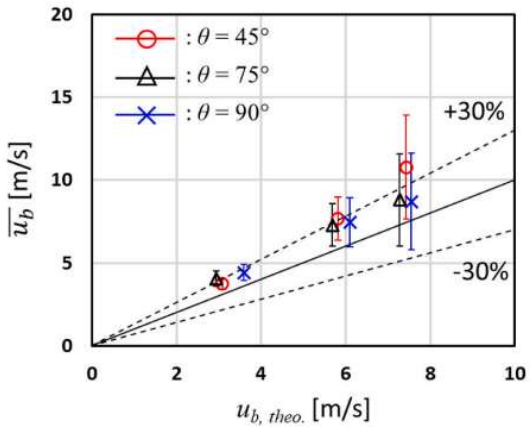

Figure 8. Mean velocity of large bubbles rising in the airlift pump

Fig. 8 shows the comparison of mean velocity of rising bubbles, u_b and the theoretical velocity of large bubble. A black solid line indicates the one-to-one correspondence between u_b and theoretical one. The dashed lines indicate the difference between both velocities. The difference is almost within ±30%, and the difference mainly comes from the different flow patterns

between the present study and Bendiksen study[13]. Many dispersed small bubbles in the slug and churn patterns were observed in the present study, Bendiksen study was completed with the little small bubbles. We supposed that the dispersed bubbles in the upside and downside of large bubbles cause the pressure difference resulting in the high variation of velocity for the large bubbles. The air flow rate of the large bubbles is next obtained using the information on u_b.

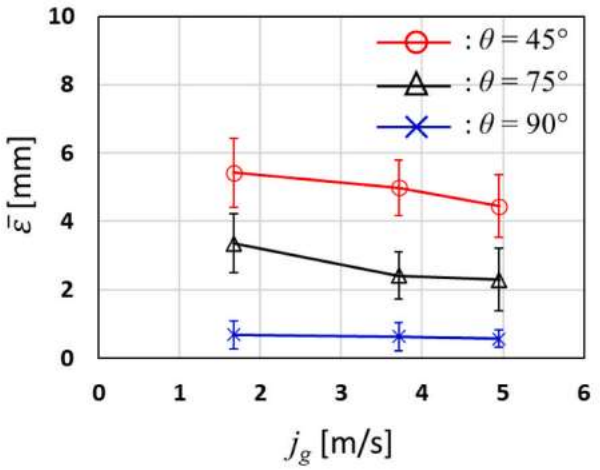

Figure 9. Mean thickness of liquid film clinging on the pipe wall

Fig. 9 shows the mean liquid film thickness of large bubbles, for each θ and j_g. It increases with the reduction of θ owing to the buoyancy contribution to the bubble; however, it tends to decrease with an increase in j_g. This is because the inertia of the gas phase flow is intensified with an increase in high j_g resulting in an increase in u_b in the streamwise direction. In other words, the buoyancy contribution weakens relative to the inertia. Note that the error bars in the figure means standard deviation come from intermittent passage of liquid slugs. Although ε slightly varies along the perimeter of the pipe, it is almost constant under the vertical condition. The volume of a large bubble rising under the vertical condition is thus easily estimated by assuming that the shape of the bubble is a cylinder.

4. Concluding Remarks

This study proposed a US measurement technique for measuring slug flow with high superficial velocities of gas–phase flow. Two methods were used to identify large bubbles in the slug flow. One used the echo intensity and the other used the Doppler frequency. It was confirmed that the method using the echo intensity was unlikely to detect a large bubble when there was scattered reflection from the uneven interface, whereas the method using the Doppler frequency could not identify a large bubble when the liquid film contained small bubbles. The two methods were thus combined to overcome their demerits, And and OR algorithms were adopted for the combined method.

Acknowledgement

This work was performed with funding from the Japan Organization for Metals and Energy Security (JOGMEC), Ministry of Economy Trade and Industry, Japanese Government (METI). The research also received funding from the JSPS KAKENHI (grant number JP21J11854). The authors are grateful to Dr. Stéphane Fischer for technical support in the use of UB-LAB X8 during the experiment and also to Prof. Yasushi Takeda for the technical advises.

References

[1] Z. Wang, Y. Kong, D. Li, X. Wang, D. Hu, Investigating the hydrodynamics of airlift pumps by wavelet packet transform and the recurrence plot" Exp, Thermal Fluid Science 92 (2018) 56–68.

[2] H. Fujimoto, T. Nagatani, H. Takuda, Performance characteristics of a gas–liquid–solid airlift pump" Int, J. Multiphase Flow 31 (2005) 1116–1133.

[3] K. Shimizu, S. Takagi, Study on the performance of a 200 m airlift pump for water and highly viscous shear-thinning slurry" Int, J. Multiphase Flow 142 (2021), 103726.

[4] Y. Murai, T. Hayashi, D. Yoon, H.J. Park, Y. Tasaka, S. Takano, S. Masanobu, Ultrasound Doppler measurement of air-lift two-phase and particulate three-phase pipe flows" Exp, Fluid 63 (2022) 126.

[5] C. Tan, Y. Murai, W. Liu, Y. Tasaka, F. Dong, Y. Takeda, Ultrasonic Doppler technique for application to multiphase flows: a review" Int, J. Multiphase Flow 144 (2021), 103811.

[6] Y. Murai, Y. Tasaka, T. Nambu, Y. Takeda, S.R. Gonzalez, Ultrasonic detection of moving interfaces in gas-liquid two-phase flow" Flow Meas, Instrumentation 21 (2010) 356–366.

[7] H.J. Park, Y. Tasaka, Y. Murai, Bubbly drag reduction investigated by time-resolved ultrasonic pulse echography for liquid films creeping inside a turbulent boundary layer" Exp, Thermal Fluid Sci 103 (2019) 66–77.

[8] H. Murakawa, H. Kikura, M. Aritomi, Application of ultrasonic multi-wave method for two-phase bubbly and slug flows" Flow Meas, Instrumentation 19 (2008) 205–213.

[9] D. Yoon, H.J. Park, T. Ihara, Development of an instantaneous velocity-vector-profile method by using conventional ultrasonic transducers" Meas, Sci. Technol. 33 (2021), 035301.

[10] H.J. Park, D. Yoon, S. Akasaka, Y. Tasaka, Y. Murai, Gas volume estimation in a vertical pipe flow considering the bubble size obtained from an ultrasonic velocity vector profiler" Exp, Fluid 63 (2022) 130.

[11] D. Yoon, T. Hayashi, H. Park, Y. Tasaka, Y. Murai, S. Takano, S. Masanobu, "Ultrasound measurement of large bubbles rising in angled slug pipe flows" Flow Measurement and Instrumentation 91 (2023) 102357.

[12] N. Otsu, A threshold selection method from gray-level histograms" IEEE, Trans. Sys. Man. Cyber. 9 (1979) 62–66.

[13] K.H. Bendiksen, An experimental investigation of the motion of long bubbles in inclined tubes, Int. J. Multiphase Flow 10 (1984) 467–483.